

## Optimum areal coverage for perfect transmission in a periodic metal hole array

J. W. Lee,<sup>1,a)</sup> T. H. Park,<sup>2</sup> Peter Nordlander,<sup>2</sup> and Daniel M. Mittleman<sup>3</sup>

<sup>1</sup>Nanophotonics Laboratory, Advanced Photonics Research Institute, GIST, Gwangju 500-712, Republic of Korea

<sup>2</sup>Department of Physics and Astronomy, Rice University, 6100 Main Street, Houston, Texas 77005, USA

<sup>3</sup>Department of Electrical and Computer Engineering, Rice University, 6100 Main Street, Houston, Texas 77005, USA

(Received 19 July 2010; accepted 7 December 2010; published online 30 December 2010)

We investigate the conditions for perfect transmission of terahertz radiation in periodic two-dimensional plasmonic system of square holes. Changing the period in the direction perpendicular to the incident light polarization reveals the *optimum areal coverage* for perfect transmission at a specific period. The simulated near-zone energy flow distributions show that all incident light is accumulated on the apertures, under the condition that the period is shorter than the resonant wavelength, acting as static local capacitors restricted to a wavelength-confined region. Our finding can be exploited for designing cost-effective terahertz filters and may be applicable to terahertz spectroscopy requiring strong local field enhancement. © 2010 American Institute of Physics. [doi:10.1063/1.3533658]

Focusing and manipulating electromagnetic fields to achieve high transparency through perforated metal films have attracted increasing attention in recent years due to promising applications in a variety of electronic, photonic, and biotechnology applications.<sup>1–3</sup> Exploiting the field enhancement of electromagnetic waves caused by resonant excitation of surface plasmons (SPs) at metal-dielectric interfaces is the best way to realize high transparency. In this case, all incident light is totally transmitted through the apertures, usually at specific frequencies. Such enhanced optical transmission has been studied in the optical frequency range<sup>4–6</sup> as well as extended to include microwave and terahertz frequencies by means of new concept such as designer SPs.<sup>7–12</sup> Particularly in the terahertz regime, near perfect transmission was experimentally realized in various types of plasmonic structures since most metals become highly conductive and consequently the Ohmic loss is small.<sup>13–16</sup> However, the rational design of efficient and feasible plasmonic structures still remains a major challenge.

In this letter, we investigate the conditions for perfect transmission through periodic two-dimensional arrays of square holes with different periods along the x- and y-axes. We propose a practical design for plasmonic structures with high transmission efficiency. Our experimental results show that the change of periodicity along the x-axis (the polarization axis of the incident wave) does not lead to a rapid decrease of the resonant transmission. Thus, structures exhibit near-unity transmission peaks over a rather wide range of array periods, in spite of the fact that spectral widths vary considerably. In contrast, when the array period along the y-axis is larger than the resonant wavelength, the peak amplitude of the transmitted terahertz waves decreases rapidly. These results strongly suggest that, for a given period, we can specify an *optimum areal coverage*, defined as the smallest fraction between the area of the apertures and the area of the metal film which maintains near-unity transmittance over

an extended wavelength regime. This can be understood from a local capacitor model in which each aperture acts as a static local capacitor restricted to a wavelength-confined region.<sup>17</sup> Simulations showing the near-zone energy flow distributions reveal that, in those cases, all impinging light is perfectly funneled through the apertures.

In order to realize plasmonic structures that can be simply understood, we fabricate two-dimensional arrays of square holes with different periods. These are drilled into a 17- $\mu\text{m}$ -thick aluminum film using a laser machining method based on amplified Ti:sapphire laser pulses. The square hole width is selected to be  $a=200\ \mu\text{m}$ . The period of the hole arrays is fixed at 400  $\mu\text{m}$  along one direction and is varied from 300 to 600  $\mu\text{m}$  with the step size of 50  $\mu\text{m}$  along the other direction. Figure 1(a) shows examples of scanning electron microscopy (SEM) images of several samples perforated with different array periods. The transmission spectra of the samples were measured using a terahertz time-domain spectroscopy system, covering the spectral range from 0.05 to 2.5 THz (wavelength range from 120  $\mu\text{m}$  to 6 mm).<sup>18–20</sup> The details of our experimental setup have been described in our previous work.<sup>10</sup>

Figure 1 shows the normalized transmission spectra measured at normal incidence for samples with different periods,  $\Delta x$  [Figs. 1(b) and 1(c)] and  $\Delta y$  [Figs. 1(d) and 1(e)], along the x- and y-axes, respectively. In the case of changing  $\Delta x$ , as the period becomes larger, the spectral peak positions of the resonant transmission shift to longer wavelength. In addition, the spectral peaks become sharper and narrower as the hole spacing increases due to the variation of the coupling between the localized SP modes of the apertures and the excitation of surface waves on the periodic structure. The normalized amplitude spectra [Fig. 1(b)] show a slight decrease due to the limit of spectral resolution related to finite sample size, sample inhomogeneity, and finite spectral resolution. Nonetheless, the near-unity transmission peaks remain over a quite wide period. Theoretical calculations [Fig. 1(c)], assuming a perfectly conducting metal film, support

<sup>a)</sup>Electronic mail: leejwc@gist.ac.kr.

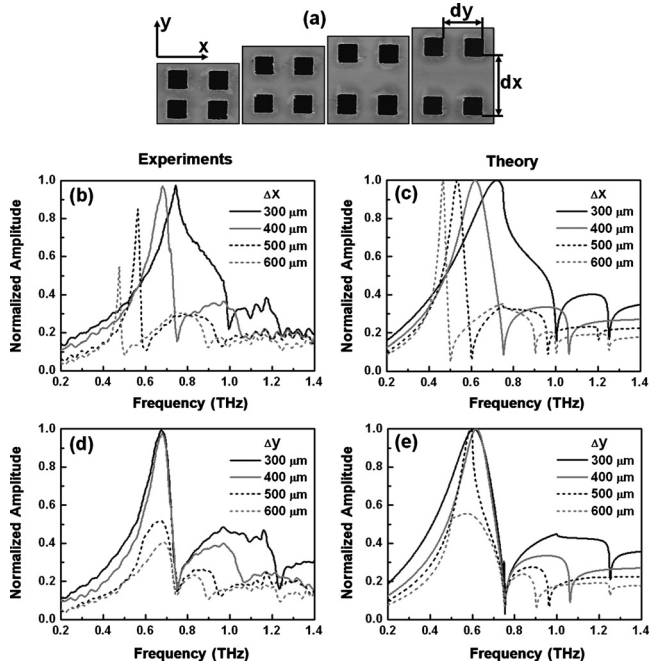


FIG. 1. (a) SEM images of the plasmonic structures perforated with different periods: 300, 400, 500, and 600 μm from left to right. Measured and calculated transmission spectra at normal incidence for four samples with different periods, 300, 400, 500, and 600 μm along x [(b) and (c)] and y [(d) and (e)] directions, respectively.

the fact that the incident light can be perfectly transmitted through the structures.<sup>21</sup> In the case of changing Δy, the resonant transmission spectra remain the same peak position shown in Figs. 1(d) and 1(e). Note that the peak values of the measured and calculated transmission amplitude spectra exhibit rapid decreases at around Δy=400 and 500 μm, respectively.

By comparing the measured and calculated peak values, we can get a further understanding of the underlying mechanism. Figure 2(a) shows the resonant peak values of the normalized transmission amplitude spectra as a function of Δy

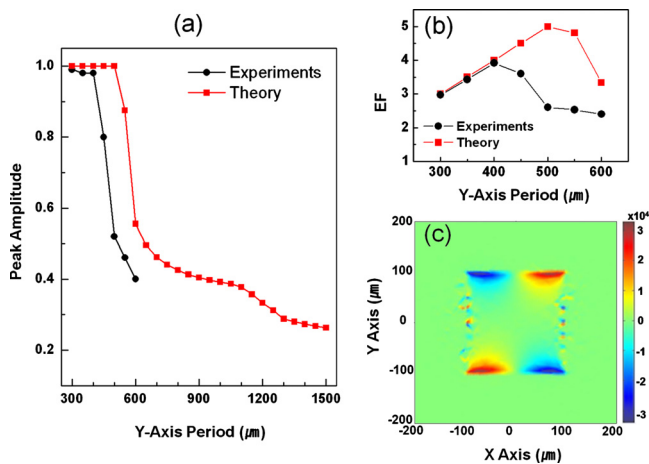


FIG. 2. (Color online) (a) The measured (black circles) and calculated (red squares) peak amplitudes at resonant frequencies. The measurements were carried out by using the samples with the Δy varying from 300 to 600 μm in an increment of 50 μm. The perfect conductor model was applied for obtaining the theoretical results. (b) The area-normalized EF. (c) Simulated  $E_y$  field distribution in the xy plane of a sample with periods of  $\Delta x, \Delta y = 400 \mu\text{m}$ . The simulation was carried out at the resonant wavelength of 490 μm. The incident polarization is along the x-axis.

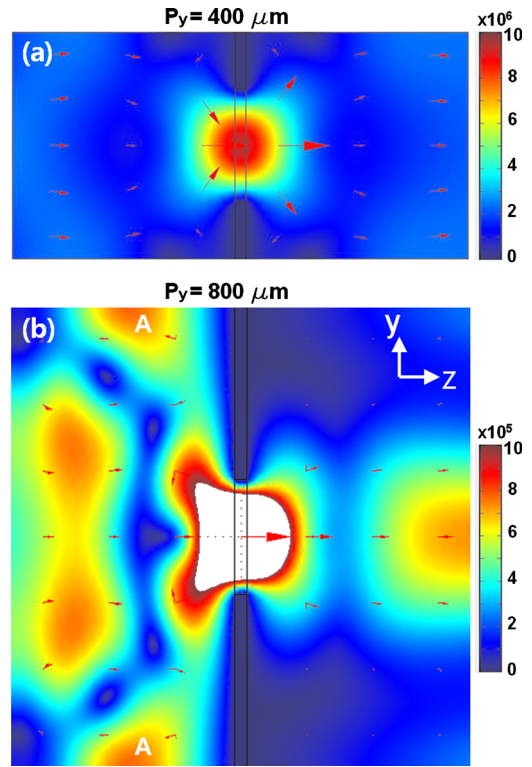


FIG. 3. (Color online) Time-averaged Poynting vectors simulated at the resonant wavelength of 490 μm for two different Δy of 400 and 800 μm, respectively. The polarization of the incident terahertz wave is along the x-direction.

(direction perpendicular to the incident polarization axis). The experimental values (black circles) of the peak amplitude transmission start to rapidly decrease at around Δy = 400 μm. Comparing the area-normalized enhancement factor (EF),  $EF = (\Delta x \Delta y / a^2) T_{\text{nor}}$ , where  $T_{\text{nor}}$  is a resonant peak value of normalized transmission electric field amplitude spectra, reveals a remarkable feature of the transmission spectra, as shown in Fig. 2(b). We note that the enhancement factor obtained from the experimental data is maximized at Δy=400 μm, which can be therefore defined as optimum Δy at which the periodic structure of holes has optimum areal coverage. The essential feature of the measured transmission spectra is reproduced by the theoretical results (red squares), even though there is a small quantitative difference in the critical period. This may be attributed to a number of factors including the finite size of the structured area and imperfect square shape of the apertures due to fabrication errors.

To understand this behavior, we performed simulations using finite element method. Figure 2(c) shows a simulation snapshot of the  $E_y$  field distribution in the xy plane of a sample with periods of  $\Delta x, \Delta y = 400 \mu\text{m}$  carried out at the resonant wavelength of 490 μm. We note that, even though the incident wave polarization is along the x-axis, there exists a near-field confinement of the  $E_y$  field at the edges lying perpendicular to the y-axis. This leads us to expect that the structure can induce oscillating electric current in the direction perpendicular to the incident wave polarization.

Computing the Poynting vector representing the flow of energy is useful for understanding a strong energy funneling associated with the strong near-field confinement. Figure 3 shows the time-averaged Poynting vectors simulated at the resonant wavelength of 490 μm for two different Δy of 400

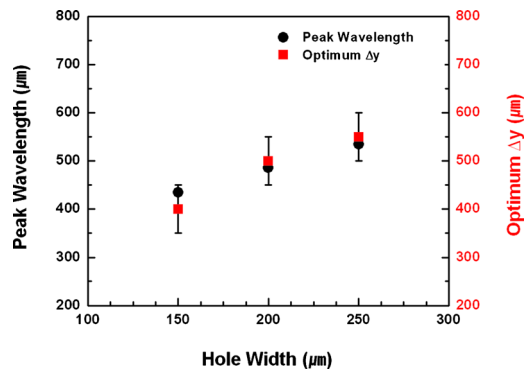


FIG. 4. (Color online) The comparison between the calculated optimum  $\Delta y$  and the resonant wavelengths obtained in the structures with the apertures of three different widths, 150, 200, and 250  $\mu\text{m}$ , respectively.

and 800  $\mu\text{m}$ . In Fig. 3(a), all the incident light is funneled through the aperture, which will enable perfect transmission. However, in the case that  $\Delta y$  is larger than the optimum  $\Delta y$  [Fig. 3(b)], a part of the energy flow which does not interact with the square holes appears on the metal surface far from the apertures, marked “A” in Fig. 3(b). This explains why perfect transmission cannot be observed in such structures and the transmission spectra show a rapid decrease of the resonant peak amplitude.

We can also understand this behavior using the concept of a “ $\lambda$ -zone” capacitance for plasmonic systems. The  $\lambda$ -zone capacitor can be defined as a static local capacitor, which induces the surface current flow inside a confined area of a diameter equal to one resonant wavelength of the incident electromagnetic wave, the so-called  $\lambda$ -zone.<sup>17</sup> Here, the local charges at the edges of the apertures can be induced by the surface current due to the law of charge conservation. Since the incident electromagnetic wave usually excites an alternating current, only the surface current oscillating in a wavelength-confined area can contribute to charging the electric carriers at the edges of the apertures. For that reason, it is important to understand the relationship between the resonant wavelength determining the  $\lambda$ -zone area and optimum  $\Delta y$ . As shown in Fig. 4, we compare the resonant wavelengths and the optimum  $\Delta y$  on the apertures of three different widths. The rather good agreement on these two spectral length scales supports the validity of this simple concept. In other words, the portion of the electromagnetic wave incident onto each  $\lambda$ -zone is totally funneled inside the corresponding aperture. The peak amplitude of the transmitted light starts to rapidly decrease when  $\Delta y$  becomes larger than the size of the  $\lambda$ -zone (i.e., the resonant wavelength).

In conclusion, we have studied the influence of the periodicity on the resonant transmission through periodic two-

dimensional plasmonic metal hole arrays. We have described an approach for minimizing the areal coverage, while maintaining perfect transmission at specific frequencies. We found that the optimum areal coverage is obtained at the optimum  $\Delta y$  which corresponds to the resonant wavelength of the plasmonic structures. A simple and intuitive  $\lambda$ -zone capacitor model provides physical insight into these experimental results and is supported by theoretical simulations of energy flow distributions in the near-field region. The physical understanding provided by this result might be important for developing terahertz plasmonic devices, satisfying the need for improved characteristics and cost-effective manufacture.

This research has been supported in part by the Photonics 2020 research project through a grant provided by the GIST in 2010, the APRI Research Program of GIST, and the National Science Foundation.

- <sup>1</sup>W. L. Barnes, A. Dereux, and T. W. Ebbesen, *Nature (London)* **424**, 824 (2003).
- <sup>2</sup>M. A. Seo, H. R. Park, S. M. Koo, D. J. Park, J. H. Kang, O. K. Suwal, S. S. Choi, P. C. M. Planken, G. S. Park, N. K. Park, Q. H. Park, and D. S. Kim, *Nat. Photonics* **3**, 152 (2009).
- <sup>3</sup>A. H. J. Yang, S. D. Moore, B. S. Schmidt, M. Klug, M. Lipson, and D. Erickson, *Nature (London)* **457**, 71 (2009).
- <sup>4</sup>T. W. Ebbesen, H. J. Lezec, H. F. Ghaemi, T. Thio, and P. A. Wolff, *Nature (London)* **391**, 667 (1998).
- <sup>5</sup>J. A. Porto, F. J. Garcia-Vidal, and J. B. Pendry, *Phys. Rev. Lett.* **83**, 2845 (1999).
- <sup>6</sup>K. J. K. Koerkamp, S. Enoch, F. B. Segerink, N. F. van Hulst, and L. Kuipers, *Phys. Rev. Lett.* **92**, 183901 (2004).
- <sup>7</sup>D. Qu, D. Grischkowsky, and W. Zhang, *Opt. Lett.* **29**, 896 (2004).
- <sup>8</sup>H. Cao and A. Nahata, *Opt. Express* **12**, 3664 (2004).
- <sup>9</sup>J. Gómez Rivas, M. Kuttge, P. Haring Bolivar, and H. Kurz, *Phys. Rev. Lett.* **93**, 256804 (2004).
- <sup>10</sup>J. W. Lee, M. A. Seo, D. S. Kim, S. C. Jeoung, Ch. Lienau, J. H. Kang, and Q.-H. Park, *Appl. Phys. Lett.* **88**, 071114 (2006).
- <sup>11</sup>J. B. Pendry, L. Martín-Moreno, and F. J. Garcia-Vidal, *Science* **305**, 847 (2004).
- <sup>12</sup>J. Han, X. Lu, and W. Zhang, *J. Appl. Phys.* **103**, 033108 (2008).
- <sup>13</sup>J. W. Lee, M. A. Seo, J. Y. Sohn, Y. H. Ahn, D. S. Kim, S. C. Jeoung, Ch. Lienau, and Q. H. Park, *Opt. Express* **13**, 10681 (2005).
- <sup>14</sup>M. Tanaka, F. Miyamaru, M. Hangyo, T. Tanaka, M. Akazawa, and E. Sano, *Opt. Lett.* **30**, 1210 (2005).
- <sup>15</sup>J. W. Lee, M. A. Seo, D. J. Park, S. C. Jeoung, Q. H. Park, Ch. Lienau, and D. S. Kim, *Opt. Express* **14**, 12637 (2006).
- <sup>16</sup>J. W. Lee, M. A. Seo, D. H. Kang, K. S. Khim, S. C. Jeoung, and D. S. Kim, *Phys. Rev. Lett.* **99**, 137401 (2007).
- <sup>17</sup>J. H. Kang, D. S. Kim, and Q. H. Park, *Phys. Rev. Lett.* **102**, 093906 (2009).
- <sup>18</sup>M. van Exter and D. Grischkowsky, *Appl. Phys. Lett.* **56**, 1694 (1990).
- <sup>19</sup>Z. Jiang, M. Li, and X. C. Zhang, *Appl. Phys. Lett.* **76**, 3221 (2000).
- <sup>20</sup>G. Zhao, R. N. Schouten, N. van der Valk, W. Th. Wenckebach, and P. C. M. Planken, *Rev. Sci. Instrum.* **73**, 1715 (2002).
- <sup>21</sup>D. J. Park, S. B. Choi, Y. H. Ahn, Q. H. Park, and D. S. Kim, *J. Korean Phys. Soc.* **54**, 64 (2009).